The 30–70 day oscillations in the tropical Atlantic

Gregory R. Foltz and Michael J. McPhaden
Pacific Marine Environmental Laboratory, NOAA, Seattle, Washington, USA

Received 18 March 2004; accepted 9 July 2004; published 11 August 2004.

[1] Evidence is presented for intraseasonal oscillations in the trade winds of the northern and southern tropical Atlantic. The pattern of intraseasonal oscillations in surface pressure and wind speed in the Northern Hemisphere resembles that of the North Atlantic Oscillation (NAO). Like the NAO, these oscillations have a strong seasonal cycle, with a maximum amplitude in boreal winter/spring. Winds in the southern tropical Atlantic are related to the Southern Hemisphere equivalent of the NAO, exhibiting a weaker seasonality with peak amplitudes in austral winter. The Madden-Julian Oscillation (MJO), which originates over the Indian Ocean, also exerts an influence on tropical Atlantic surface winds, particularly between about 10°N and 10°S. Where intraseasonal wind speed oscillations in the Atlantic are strong, they force changes in sea surface temperature (SST) through latent heat loss from the ocean, potentially affecting lower frequency climate variations. *INDEX TERMS:* 4504 Oceanography: Physical: Air/sea interactions (0312); 3339 Meteorology and Atmospheric Dynamics: Ocean/atmosphere interactions (0312, 4504); 3374 Meteorology and Atmospheric Dynamics: Tropical meteorology; 4572 Oceanography: Physical: Upper ocean processes. **Citation:** Foltz, G. R., and M. J. McPhaden (2004), The 30–70 day oscillations in the tropical Atlantic, *Geophys. Res. Lett.*, *31*, L15205, doi:10.1029/2004GL020023.

1. Introduction

[2] The climates of the tropical Atlantic and tropical Pacific are similar in many respects. Common features include the seasonal appearance of a tongue of cool SST along and south of the equator and predominantly easterly surface winds. On time scales longer than the seasonal cycle, however, there are important differences. Whereas variability in the tropical Pacific is dominated by zonal shifts of heat and convection close to the equator, variability in the tropical Atlantic contains a significant meridional mode that extends into the subtropics [*Nobre and Shukla*, 1996]. On decadal time scales, much of this variability can be attributed to thermodynamic interactions between the tropical Atlantic Ocean and the overlying atmosphere [*Chang et al.*, 1997]. Recent studies suggest that this coupled air-sea oscillation cannot sustain itself, implying that external forcing, possibly from the equatorial Pacific or the North Atlantic, plays an important role [*Saravanan and Chang*, 2000; *Chang et al.*, 2001]. The nature and strength of interactions between the extratropical and tropical Atlantic, however, remain unclear [*Xie and Tanimoto*, 1998; *Wu and Liu*, 2002]. Here we present evidence of intraseasonal (30–70 day) oscillations in the tropical Atlantic, which may contribute to the phasing and intensity of longer time scale variability.

0094-8276/04/2004GL020023$05.00

2. Data

[3] This study is based on the analysis of several near-surface oceanic and atmospheric data sets and satellite outgoing longwave radiation (OLR). Weekly SST was obtained from a blended satellite-in situ product [*Reynolds et al.*, 2002] for the period 1982–2002 and interpolated to a daily resolution. Daily surface (10 m) wind velocity and surface atmospheric pressure are available from the NCEP/NCAR reanalysis [*Kalnay et al.*, 1996] for the period 1948 to the present. For coincident analysis with the *Reynolds et al.* [2002] SST data set, we use the reanalysis from 1982–2002 only. Daily near-surface wind speed (at a height of 4 m), relative humidity (3 m), air temperature (3 m), and SST (at a depth of 1 m) for the period 1998–2002 were obtained from the two most poleward moored buoys of the Pilot Research Array in the Tropical Atlantic (PIRATA) [*Servain et al.*, 1998] located at 15°N, 38°W, 10°S, 10°W. As a proxy for deep atmospheric convection, we use daily OLR from the NOAA polar orbiting satellites, available from the NOAA-CIRES Climate Diagnostics Center for the period 1982–2002. A daily mean seasonal cycle was removed from each data set, and the resultant data were band-passed to emphasize periods of 30–70 days. We also use daily winds measured by the SeaWinds scatterometer aboard the QuikSCAT satellite (1999–2002) for comparison with the NCEP/NCAR reanalysis and PIRATA winds (Figure 1).

3. Results

[4] Surface wind speed plays an important role in seasonal and longer time scale variability in the tropical Atlantic through its effect on latent heat loss from the ocean and hence SST [*Carton et al.*, 1996; *Foltz et al.*, 2003]. We find that there is substantial wind speed variability on intraseasonal time scales in the northern and southern tropics within the northeasterly and southeasterly trade winds, respectively. Spectral analyses of the unfiltered NCEP/NCAR reanalysis wind speed over broad areas reveal enhanced variance in the 30–70 day period range relative to a red noise spectrum. A pronounced peak centered near 55 days is evident in the northern tropics during 1999–2002, consistent with both contemporaneous mooring and satellite scatterometer wind estimates (Figure 1). There is also a peak (significant at the 75% level) centered near 50 days in the southern tropical wind speed spectra during the same time period (not shown).

[5] We define two index regions in which the percentage of the variance in the 30–70 day band is highest (Figure 2),

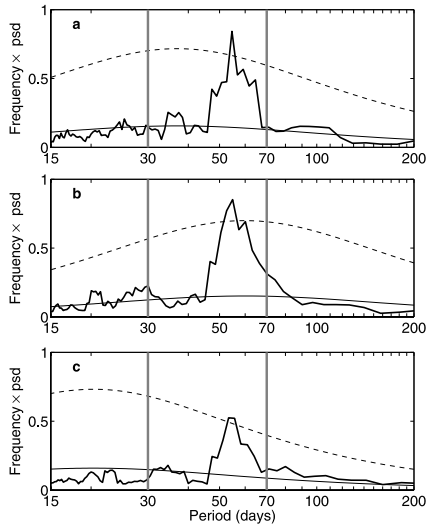

Figure 1. (a) Normalized power spectrum of NCEP/NCAR reanalysis daily wind speed in the NATL index region (Figure 2a) for the period 1999–2002. (b) Same as in (a), except for daily QuikSCAT wind speed. (c) Same as in (a), except for wind speed from the PIRATA buoy at 15°N, 38°W (Figure 2a). PIRATA and QuikSCAT data were smoothed with a 10-day running mean to fill gaps, and the NCEP/NCAR reanalysis data were also smoothed for consistency (the origin of the x-axis is therefore 15 days in all plots). Spectra are shown as variance-preserving plots. Solid black lines represent red noise spectra based on a lag-1 autoregressive process [*Gilman et al.*, 1963]. Dashed lines represent the 90% confidence level of a chi-square distribution. Vertical gray lines indicate periods of 30 and 70 days.

namely 15°N–25°N, 20°W–50°W (designated NATL) and 10°S–20°S, 0°–30°W (designated SATL). Variability in the 30–70 day band accounts for 17% of the total daily wind speed variance (1982–2002) in the NATL region and 15% in the SATL region. These high percentages are matched only in the tropical Indo-Pacific, where surface fluctuations associated with the MJO are strongest. The amplitudes of the NATL and SATL wind speed oscillations are typically ±1 m s^{-1} (Figure 2). The NATL oscillation is strongest in boreal winter (Figure 3a), while the SATL oscillation shows a weaker seasonal dependence, with a maximum in boreal summer (Figure 3b). There is also considerable year-to-year variability in these wind speed oscillations (Figures 2b and 2c).

[6] To examine the surface conditions associated with the NATL and SATL oscillations, we have performed a linear regression of NCEP/NCAR reanalysis wind velocity and atmospheric pressure and *Reynolds et al.* [2002] SST to the NATL and SATL indices. Oscillations of the NATL index are associated with anomalous surface pressure centered near 35°N, 35°W and 60°N, 20°W, each with corresponding geostrophic surface wind anomalies (Figure 4a). These surface pressure and wind patterns resemble those of the North Atlantic Oscillation (NAO), which is the dominant wintertime interannual-to-decadal atmospheric signal in the North Atlantic [*Hurrell*, 1995]. The strongest wind speed anomalies (up to 3 m s^{-1}) occur along 20°N–25°N in the central basin (Figure 4b). In general, the regions of strong wind speed anomalies correspond to areas of strong SST anomalies, with SST generally lagging by about two weeks. This phasing suggests that on intraseasonal time scales, the atmosphere may force the ocean through the effect of changes in wind speed on latent heat loss. The NCEP/NCAR reanalysis does not exhibit a strong relationship between wind speed and latent heat flux in this region, most likely because surface heat fluxes are one of the most poorly represented fields in the reanalysis [*Kalnay et al.*, 1996]. However, measurements from the PIRATA buoy at 15°N, 38°W, just south of the strongest 30–70 day wind speed variability (Figure 4b), reveal high correlations between $\partial(SST)/\partial t$ and latent heat loss (−0.75) and between latent heat loss and wind speed (0.84), both significant at the 99% level.

[7] The surface structure associated with oscillations of the SATL index resembles the pattern associated with oscillations of the NATL index (Figure 4c and 4d). There are regions of anomalous surface pressure centered near 35°S, 20°W and 60°S, 50°W, with corresponding patterns of near-surface wind and SST anomalies. Data from the PIRATA buoy at 10°S, 10°W show weaker SST, latent heat loss, and wind speed fluctuations and weaker cross-correlations ($|r| < 0.3$) in comparison to those observed at 15°N, 38°W. These differences may be due in part to the fact that the southern buoy is farther offset from the region

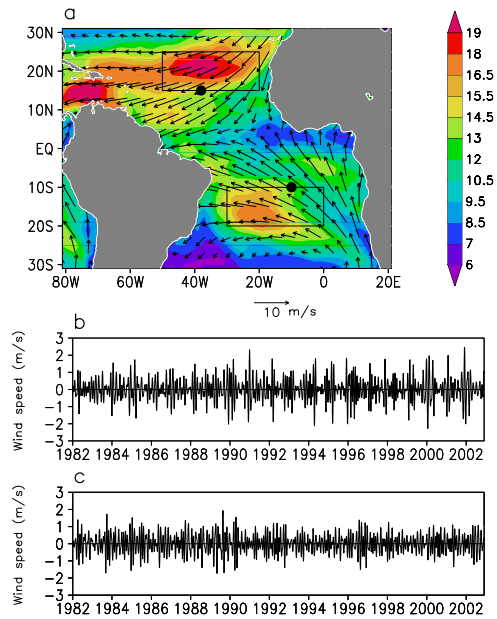

Figure 2. (a) Percentage of the total wind speed variance (1982–2002) accounted for by the 30–70 day wind speed oscillations. The spatial pattern of the total variance in the 30–70 day band is similar, but with a maximum in the northern tropics that is displaced slightly poleward and a maximum in the south that extends farther eastward. Arrows denote NCEP/NCAR reanalysis annual mean near-surface wind velocity. Rectangles in the northern and southern tropics enclose the regions used to form the NATL and SATL indices, respectively. Black dots indicate locations of the PIRATA buoys used in this study. (b) Amplitude of the 30–70 day NATL oscillations. (c) Amplitude of the 30–70 day SATL wind speed oscillations.

of strong wind speed variability in the south tropical Atlantic (Figure 4d). Correlations between NATL and SATL are <0.1 (not significantly different from zero at the 95% confidence level, based on ~275 degrees of freedom [*Crow et al.*, 1960; *Davis*, 1976]) at lags of up to 40 days in either direction, suggesting that the northern and southern oscillations are not dynamically linked.

4. Possible Relationship to the Madden-Julian Oscillation

[8] In order to investigate a possible connection between the Atlantic intraseasonal oscillations and the MJO [*Madden and Julian*, 1971], we have performed correlation and regression analyses of NCEP/NCAR reanalysis surface pressure and near-surface wind velocity with a MJO index consisting of the principal component coefficient of the first EOF of 30–70 day OLR in the eastern tropical Indian and western tropical Pacific (60°E–90°W, 30°S–30°N) [*Slingo et al.*, 1999] for the period 1982–2002. Positive values of the MJO index correspond to enhanced convection over the equatorial Indian Ocean (60°E–100°E) and reduced convection in the western equatorial Pacific (140°E–180°). We find that the MJO is significantly correlated with surface winds throughout the tropical Atlantic when the MJO leads by 10–14 days (Figure 5a). Cross-correlations with surface winds range between ~0.4 near the equator and ~0.2 at the poleward extremities of the pattern in Figure 5a. The observed lag times and spatial structures evident in Figure 5a are consistent with the results of *Matthews* [2000], which are derived from a similar OLR-based MJO index. He shows a region of low atmospheric pressure in the eastern equatorial Pacific and a pair surface anticyclones near 30°S and 30°N along 30°W 10–15 days after MJO convection over the eastern Indian Ocean reaches a maximum.

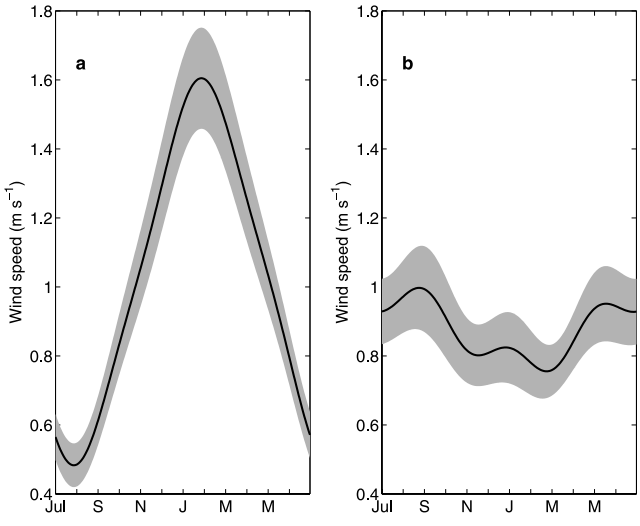

Figure 3. Seasonality of the tropical Atlantic 30–70 day wind speed anomalies. (a) Seasonal cycle (1982–2002) of the amplitude of the complex demodulation of the NATL index (calculated with a central period of 50 days). (b) Seasonal cycle of the amplitude of the complex demodulation of the SATL index. Gray shading represents one standard error, estimated using 21 degrees of freedom. Calculations with central periods of 30 days and 70 days give similar results.

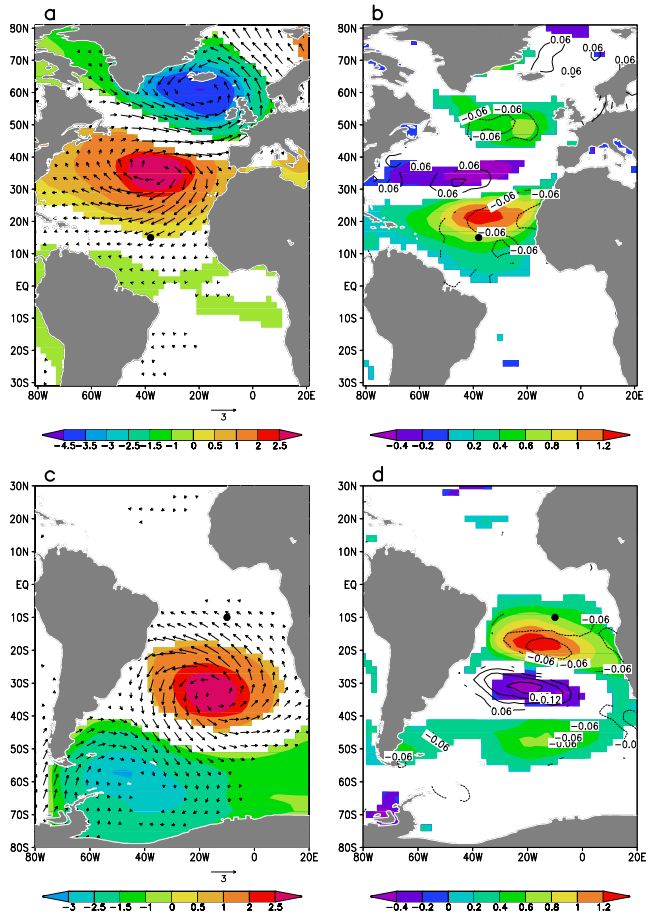

Figure 4. Surface structure of the intraseasonal oscillations based on linear regression to the NATL and SATL indexes. (a) NCEP/NCAR reanalysis surface pressure (shaded, mb (m s^{-1})$^{-1}$) and wind velocity (arrows) and (b) NCEP/NCAR reanalysis wind speed and *Reynolds et al.* [2002] SST (contours, °C (m s^{-1})$^{-1}$) regressed to the NATL index. (c) and (d): same as (a) and (b), except regressed to the SATL index. SST was regressed with a 12-day lag (i.e., SST lags NATL and SATL by approximately one quarter of a cycle). Values are shown only if they exceed the 95% confidence level [based on *Crow et al.*, 1960; *Davis*, 1976]. Wind vectors are plotted if either zonal or meridional component exceeds the 95% level. Black dots at 15°N, 38°W in (a), (b) and at 10°S, 10°W in (c), (d) indicate the locations of the PIRATA buoys used in this study.

[9] The surface pressure and wind patterns in the NATL index region resemble those patterns associated with oscillations of the NATL index itself (Figure 4a), suggesting that the MJO in the equatorial Indo-Pacific may excite some of the intraseasonal variability in the north tropical Atlantic. The fact that the NATL and SATL indices are not highly correlated despite the spatially coherent forcing from the MJO (Figure 5a) suggests that the direct influence of the MJO is a secondary factor in determining the intraseasonal variability in tropical Atlantic winds poleward of about 10°N and 10°S. Other factors, such as internal atmospheric dynamics that give rise to the NAO and its Southern Hemisphere counterpart, must exert a stronger influence

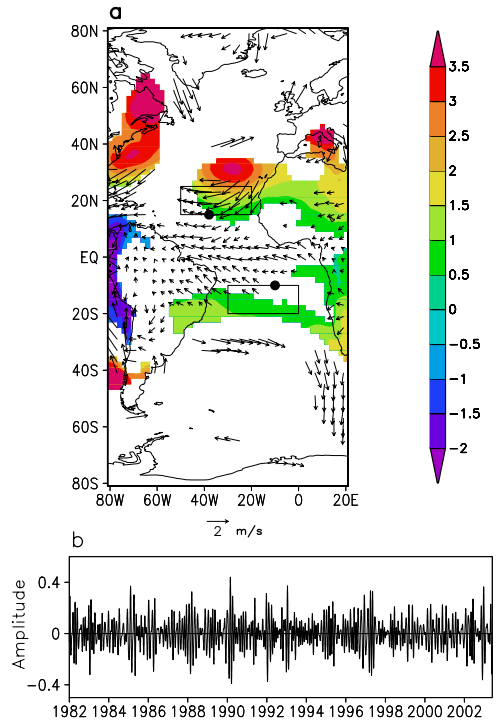

Figure 5. (a) NCEP/NCAR reanalysis surface pressure (shaded, mb) and wind velocity (arrows) regressed to the Indo-Pacific MJO index shown in (b) (MJO index leads by 10 days). Rectangles enclose the regions used to form the NATL and SATL indices, respectively. Black dots indicate the locations of the PIRATA buoys used in this study. Surface pressure is shown only where it exceeds the 95% confidence level. Wind vectors are plotted if either component exceeds the 95% level.

on the phasing and intensity of the oscillations in these regions. Indeed, the NATL wind speed index is more highly correlated with the 30–70 day band-passed NAO surface pressure index (0.3) [*Hurrell*, 1995] than with the MJO (0.2). However, the MJO may play a more prominent role in determining intraseasonal wind field variability between 10°N and 10°S (Figure 5a). Also, it is possible that the MJO has an indirect effect on tropical Atlantic winds through projection onto the NAO and its Southern Hemisphere counterpart through teleconnections from the Indian Ocean [*Ferranti et al.*, 1990; *Annamalai and Slingo*, 2001], though this effect is not apparent in Figure 5a.

5. Summary

[10] Our results show that the strengths of the trade winds in the tropical Atlantic vary considerably on time scales of one to two months. The northern and southern trade wind oscillations are associated with coherent surface wind and pressure patterns that span the entire North and South Atlantic, respectively, suggesting that midlatitude atmospheric variability contributes significantly to the intraseasonal oscillations in the tropical Atlantic poleward of about 10°N and 10°S. The oscillations in the tropical Atlantic are also significantly correlated with the MJO in the Indo-Pacific, suggesting that the MJO also exerts an influence on surface winds, particularly equatorward of 10°. We have found that the fluctuating winds in the tropical Atlantic force changes in SST through their effect on the surface latent heat flux. This atmospheric forcing mechanism has been shown to play a key role in interannual and decadal climate variations in the region, suggesting that the shorter time scale fluctuations may play a role in energizing lower frequency climate variations. Thus, just as in the Pacific, where intraseasonal oscillations play a prominent role in affecting the evolution of the El Niño/Southern Oscillation cycle [*McPhaden*, 2004], the coherent intraseasonal oscillations described in this study may play an important role in affecting the character of climate variability in the tropical Atlantic.

[11] **Acknowledgment.** This research was performed while GF held a National Research Council Research Associateship Award at NOAA/PMEL. PMEL contribution 2696.

References

Annamalai, H., and J. M. Slingo (2001), Active/break cycles: Diagnosis of the intraseasonal variability of the Asian summer monsoon, *Clim. Dyn.*, *18*, 85–102.

Carton, J. A., X. Cao, B. S. Giese, and A. M. da Silva (1996), Decadal and interannual SST variability in the tropical Atlantic Ocean, *J. Phys. Oceanogr.*, *26*, 1165–1175.

Chang, P., L. Ji, and H. Li (1997), A decadal climate variation in the tropical Atlantic Ocean from thermodynamic air-sea interactions, *Nature*, *385*, 516–518.

Chang, P., L. Ji, and R. Saravanan (2001), A hybrid coupled model study of tropical Atlantic variability, *J. Clim.*, *14*, 361–390.

Crow, E. L., F. A. Davis, and M. W. Maxfield (1960), *Statistics Manual*, Dover, Mineola, N. Y.

Davis, R. E. (1976), Predictability of sea surface temperature and sea level pressure anomalies over the North Pacific Ocean, *J. Phys. Oceanogr.*, *6*, 249–266.

Ferranti, L., T. N. Palmer, F. Molteni, and E. Klinker (1990), Tropical-extratropical interaction associated with the 30–60 day oscillation and its impact on medium and extended range prediction, *J. Atmos. Sci.*, *47*, 2177–2199.

Foltz, G. R., S. A. Grodsky, J. A. Carton, and M. J. McPhaden (2003), Seasonal mixed layer heat budget of the tropical Atlantic Ocean, *J. Geophys. Res.*, *108*, 3146, doi:10.1029/2002JC001584.

Gilman, D. L., F. J. Fuglister, and J. M. Mitchell Jr. (1963), On the power spectrum of "red noise," *J. Atmos. Sci.*, *20*, 182–184.

Hurrell, J. E. (1995), Decadal trends in the North Atlantic Oscillation: Regional temperatures and precipitation, *Science*, *269*, 676–679.

Kalnay, E., et al. (1996), The NCEP/NCAR 40-year reanalysis project, *Bull. Am. Meteorol. Soc.*, *77*, 437–471.

Madden, R. A., and P. R. Julian (1971), Detection of a 40–50 day oscillation in the zonal wind in the tropical Pacific, *J. Atmos. Sci.*, *28*, 702–708.

Matthews, A. J. (2000), Propagation mechanisms for the Madden-Julian oscillation, *Q. J. R. Meteorol. Soc.*, *126*, 2637–2651.

McPhaden, M. J. (2004), Evolution of the 2002–03 El Niño, *Bull. Am. Meteorol. Soc.*, *85*, 677–695.

Nobre, C., and J. Shukla (1996), Variations of sea surface temperature, wind stress, and rainfall over the tropical Atlantic and South America, *J. Clim.*, *9*, 2464–2479.

Reynolds, R. W., N. A. Rayner, T. M. Smith, D. C. Stokes, and W. Q. Wang (2002), An improved in situ and satellite SST analysis for climate, *J. Clim.*, *15*, 1609–1625.

Saravanan, R., and P. Chang (2000), Interaction between tropical Atlantic variability and El Niño–Southern Oscillation, *J. Clim.*, *13*, 2177–2194.

Servain, J., A. J. Busalacchi, M. J. McPhaden, A. D. Moura, G. Reverdin, M. Vianna, and S. E. Zebiak (1998), A pilot research moored array in the tropical Atlantic (PIRATA), *Bull. Am. Meteorol. Soc.*, *79*, 2019–2031.

Slingo, J. M., D. P. Rowell, K. R. Sperber, and F. Nortley (1999), On the predictability of the inter annual behavior of the Madden-Julian oscillation and its relationship with El Niño, *Q. J. R. Meteorol. Soc.*, *125*, 583–609.

Wu, L., and Z. Liu (2002), Is tropical Atlantic variability driven by the North Atlantic Oscillation?, *Geophys. Res. Lett.*, *29*, 1653, doi:10.1029/2002GL014939.

Xie, S.-P., and Y. Tanimoto (1998), A pan-Atlantic decadal climate oscillation, *Geophys. Res. Lett.*, *25*, 2185–2188.

G. R. Foltz and M. J. McPhaden, Pacific Marine Environmental Laboratory, NOAA, 7600 Sand Point Way NE, Seattle, WA 98115, USA. (gregory.foltz@noaa.gov)